ACS OMEGA

http://pubs.acs.org/journal/acsodf

Article

Benzo[*b*]selenophene/thieno[3,2-*b*]indole-Based N,S,Se-Heteroacenes for Hole-Transporting Layers

Nadezhda S. Demina, Nikolay A. Rasputin, Roman A. Irgashev,* Alexey R. Tameev,* Natalia V. Nekrasova, Gennady L. Rusinov, Jean-Michel Nunzi, and Valery N. Charushin

Cite This: *ACS Omega* 2020, 5, 9377−9383

Read Online

ACCESS | Metrics & More | Article Recommendations | Supporting Information

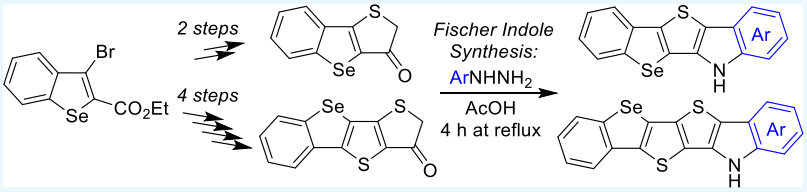

ABSTRACT: Two series of new N,S,Se-heteroacenes, namely, 6*H*-benzo[4′,5′]selenopheno[2′,3′:4,5]thieno[3,2-*b*]indoles and 12*H*-benzo[4″,5″]selenopheno[2″,3″:4′,5′]thieno[2′,3′4,5]thieno[3,2-*b*]indoles, were successfully obtained using an effective strategy based on Fiesselmann thiophene and Fischer indole synthesis. The new molecules exhibit a large optical band gap (2.82 eV < E_g^{opt} < 3.23 eV) and their highest occupied molecular orbital (HOMO) energy formed by the plane π-core ranges between −5.2 and −5.6 eV, with the narrower optical band gap and lower HOMO level corresponding to selenated heteroacenes. In thin solid films of the heteroacenes, hole mobility measured using the conventional CELIV technique ranges between 10^{-5} and 10^{-4} $cm^2 \cdot V^{-1} \cdot s^{-1}$. All these make the proposed condensed-ring compounds a promising platform for the development of hole-transporting materials applicable in organic electronics.

INTRODUCTION

Organic π-conjugated ring-fused molecules, built up from both aromatic and heteroaromatic units, are key structure elements in photo- and electroactive materials. They found many applications as active components in organic light-emitting diodes,[1−3] organic field effect transistors,[4−6] and organic photovoltaics.[7−9] Thereby, the interest of researchers all around the world in such compounds, including their design, synthesis, and properties study, is steadily increasing at a rapid pace.[10−12] Among these molecules, π-excessive heteroacenes, bearing thiophene and pyrrole rings, have been widely shown as attractive p-type semiconductors exhibiting good charge-carrier mobility as well as better environmental stability, owing to their low-lying highest occupied molecular orbital (HOMO) energy levels, in comparison with their fully carbon-cored analogous acenes.[13,14] Furthermore, a number of fused thiophene/pyrrole molecules have been successfully used as electron-donating blocks in the construction of light-harvesting materials, both push−pull small molecules and polymers, for organic photovoltaics with high power conversion efficiency.[15−19]

At the same time, selenophene-based semiconductors exhibit a number of advantageous properties as compared to their thiophene-containing counterparts: narrower optical band gap, lower oxidation and reduction potentials, and well-organized solid-state packing due to strong intermolecular Se−Se interactions, all of which overall allow enhancing the performance of organic electronics devices based on such heteroacenes.[20−22] Taking into account these data, the incorporation of selenium atoms into π-conjugated frameworks and fused compounds, intended for the use in organic electronics, is clearly a promising molecular design strategy, allowing us to improve efficiency of these functional materials.[23,24] Therefore, research efforts aiming at elaboration of new types of selenophene-containing semiconductors as well as at studying their properties are fully justified from the perspective of further optoelectronic applications. Thus, various types of heteroacenes, containing thienopyrrole,[13,18] selenophenopyrrole,[25,26] or selenophenothiophene fragments,[27,28] have previously been synthesized and used as organic electronic materials. However, there are no reports on any fused molecules with a triple combination of pyrrole, thiophene, and selenophene rings to the best of our knowledge.

Taking into account rather strong interest into new ring-fused organic molecules, we report herein on a convenient synthesis of 6*H*-benzo[4′,5′]selenopheno[2′,3′:4,5]thieno[3,2-

Received: January 27, 2020
Accepted: April 7, 2020
Published: April 17, 2020

b]indole (BTTI) and 12*H*-benzo[4″,5″]selenopheno-[2″,3″:4′,5′]thieno[2′,3′:4,5]thieno[3,2-*b*]indole (BSTTI) derivatives, depicted on Figure 1, as well as an investigation of their semiconductor properties.

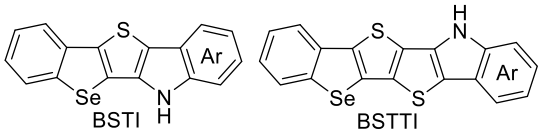

Figure 1. Structures of N,S,Se-heteroacenes.

RESULTS AND DISCUSSION

Synthesis. For access to the aforementioned N,S,Se-heteroacenes, we constructed their thieno[3,2-*b*]indole (TI) part through three-step transition-metal-free way based on the Fiesselmann thiophene synthesis and the Fischer indole synthesis as key transformations. A similar synthetic plan was recently applied by us to the synthesis of thieno[3,2-*b*]indole-based N,S-heteroacenes (BTTI) **2**[29] and 2-(hetero)aryl-substituted thieno[3,2-*b*]indoles **4**[30] from the appropriate 1,3-C,C-dielectrophilic substrates, namely, 3-chlorobenzo[*b*]-thiophene-2-carboxylates **1** and 2-bromo-3-(hetero)-arylacrylates **3**. They were used to obtain the intermediated 3-hydroxythiophen-2-carboxylates **A** via the Fiesselmann method, followed by conversion of compounds **A** to thiophen-3(2*H*)-ones **B** and the next treatment of ketones **B** with arylhydrazines to directly afford the target TI derivatives by Fischer indolization (Scheme 1).

Scheme 1. Synthetic Way to TI Compounds, Based on the Fiesselmann and Fischer Methods

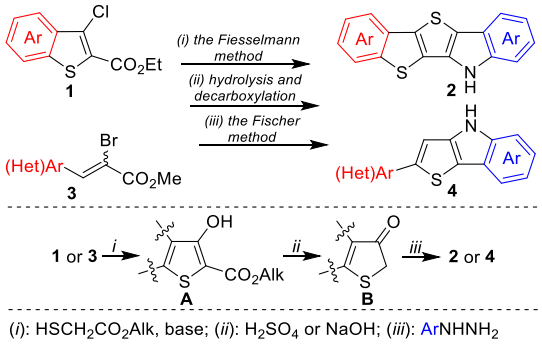

To this end, we chose a suitable benzo[*b*]selenophene (BS)-based source material to implement our synthetic method to the N,S,Se-heteroacene molecules. In this regard, our attention was drawn to a convenient one-pot synthesis of 3-bromobenzo[*b*]selenophene derivatives by the treatment of phenylacetylenes with SeO_2 and 48% aq. HBr in the presence of cyclohexene, which was previously reported by Arsenyan and co-workers.[31,32] In particular, they demonstrated cyclization of ethyl phenylpropiolate to ethyl 3-bromobenzo[*b*]-selenophene-2-carboxylate **5**. The structure of the latter molecule contains the 1,3-dielectrophilic three-carbon fragment, formed by the ethoxycarbonyl group and the C-3 position with the bromine atom, which motivated us to utilize this BS compound as the starting substrate in our synthetic strategy. Thus, compound **5** prepared using the slightly modified literature procedure[31] was condensed with ethyl thioglycolate (2 equiv) in the presence of potassium *tert*-butoxide (4 equiv) in THF medium to form fused 3-hydroxythiophene-2-carboxylate **6** in 69% yield. Next, saponification of the latter ester with sodium hydroxide in aqueous DMSO solution, followed by acidic workup of a reaction mixture to perform in situ decarboxylation of the obtained acid, afforded thiophen-3(2*H*)-one **7** in 95% yield (Scheme 2). In addition, tricyclic 3-hydroxyester **6** was also treated with triflic anhydride (Tf_2O) in the presence of bases to form its triflate derivative **8**, bearing a 1,3-C,C-dielectrophilic moiety, further needed to perform annulation of one more thiophene ring by the Fiesselmann reaction.

Synthesis of the BSTI molecules was successfully performed by the treatment of fused thienone **7** with hydrochloride of phenyl- **9a**, 4-methylphenyl- **9b**, 4-bromophenyl- **9c**, or 1-naphtylhydrazine **9d** (1.5 equiv) in the presence of anhydrous sodium acetate (1.5 equiv) in glacial acetic acid. Full indolization of initially formed arylhydrazones of ketone **7** proceeded when the reaction mixtures were being refluxed for 4 h. Thus, desired products **10a−d** were isolated in 85−90% yields (Scheme 3).

The same three-step strategy was applied for the construction of the BSTTI molecules bearing one extra thiophene unit in their frameworks. To this end, triflate derivative **8** was treated with ethyl thioglycolate (2 equiv) and potassium *tert*-butoxide (4 equiv) under the reaction conditions similar to the compound **6** synthesis, affording desired tetracyclic 3-hydroxyester **11**. However, along with normal substitution of triflate in substrate **8**, we observed that the undesirable reaction of its *o*-detriflylation was forming prior 3-hydroxyester **6**. Nevertheless, pure 3-hydroxyester **11** was obtained in 30% yield by crystallization from toluene, while side product **6** was also isolated in 28% yield after dilution of the toluene mother liquor with ethanol. Next, 3-hydroxyester **11** was converted to corresponding thiophen-3(2*H*)-one **12** in almost quantitative yield. Heteroacenes **13a−d** were obtained in 50−71% yield by the reaction of ketone **12** with

Scheme 2. Synthesis of Functional Benzo[4,5]selenopheno[3,2-*b*]thiophenes 6 and 7, 8

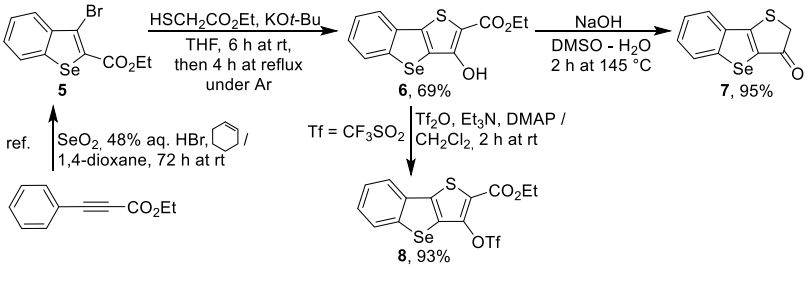

https://dx.doi.org/10.1021/acsomega.0c00383
ACS Omega 2020, 5, 9377−9383

Scheme 3. Synthesis of BSTI Derivatives 10, Substrate Scope, and Yields

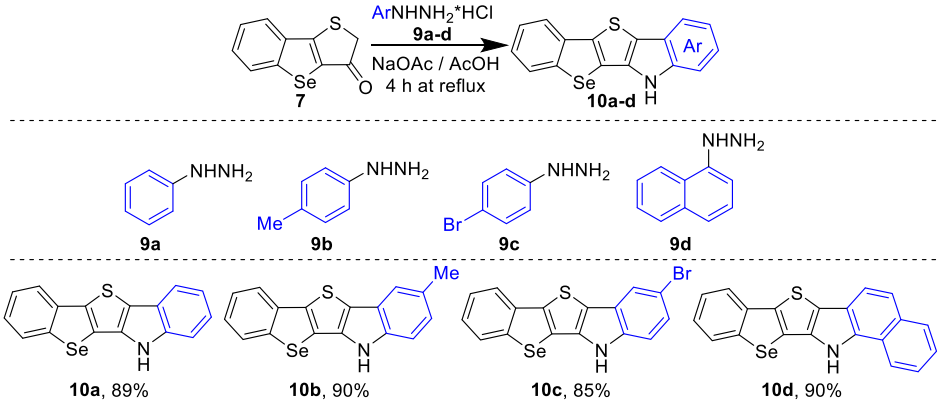

arylhydrazines **9a−d** in line with the Fischer indolization protocol (Scheme 4).

Scheme 4. Synthetic Way to BSTTI Derivatives 13, Substrate Scope, and Yields

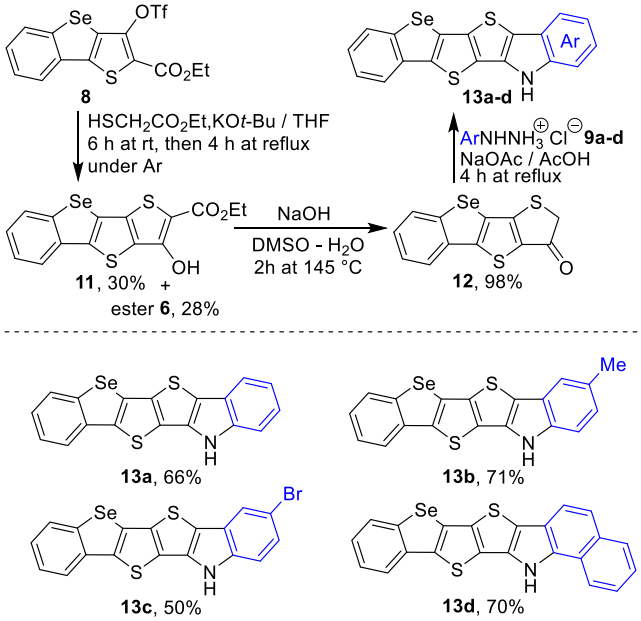

Electronic Properties of Thin Solid Layers. In this study, we investigated electronic properties of synthesized BSTI and BSTTI derivatives **10a**, **d** and **13a** as well as previously reported thiophene/pyrrole-based analogues[29] of these N,S,Se-heteroacenes, such as compounds **T-10a**, **d** and **T-13a** (Figure 2). Solubility of these compounds is low, so we could prepare solutions of N,S,Se-heteroacenes in tetrahydrofuran. The UV absorption spectra of the N,S,Se-heteroacenes in solution are presented in Figure 3a. Thin solid films of the new compounds were easily prepared using the thermal vacuum evaporation technique. Absorption spectra of the films are shown in Figure 3b. For defining the optical band gap, the absorption spectra plotted versus energy are presented in Figures S27-S29 as well. The narrower optical band gap and lower HOMO level corresponding to selenated heteroacenes (Table 1) evidently originate from stronger intermolecular Se−Se interaction compared with that of for sulfur atoms.

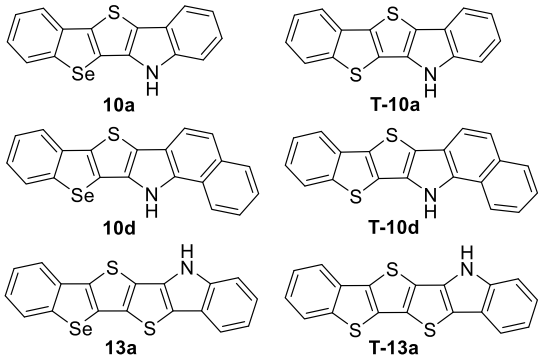

Figure 2. Structures of studied N,S,Se-heteroacenes and their N,S-counterparts.

The XRD spectra (Figure S26) show that solid layers of the N,S,Se-heteroacenes, and their N,S-counterparts consist of well-ordered domains visible as sharp diffraction peaks. Some compounds also possess an amorphous phase visible as a halo diffraction around $2\theta = 24°$. When looking more particularly at the five-ringed members of the series, they have larger mobilities than the four-ringed members, and we see that the N,S,Se-heteroacenes are more amorphous than their N,S-counterparts. We also see in Table 1 that their mobilities are larger than the more crystalline N,S-heteroacenes. Generally, the HOMO (LUMO) energy levels in the ordered domains are higher (lower) compared to those in the corresponding molecules of the amorphous phase. In an entire layer, the ordered domains act as traps for holes (electron) when they do not form a continuous single crystalline network. That is how we interpret the origin of the low CELIV hole mobilities in the order of 10^{-5} $cm^2 \cdot V^{-1} \cdot s^{-1}$ (Table 1) of the studied compounds and the differences between similar compounds; the electron mobility was lower by 1 order of magnitude at least.

Charge carrier mobility in organic materials is governed by electron hopping between neighboring molecules. It increases with the wave-function overlap between the nearest neighbors. The larger the conjugated molecule is, the larger the wavefunction overlap will be, which will lead to larger mobilities. This justifies that **10a** and **T-10a** molecules, with five condensed rings versus six ones for the other molecules, exhibit the smallest mobilities. Similarly, **10d** and **T-10d** show extended π-electron conjugation with respect to **13a** and **T-13a**, which also justifies their relatively larger mobilities. Moreover, the dipole moment of the **10d** and **T-10d** molecules is lower than that in other molecules, and this fact agrees well

https://dx.doi.org/10.1021/acsomega.0c00383
ACS Omega 2020, 5, 9377−9383

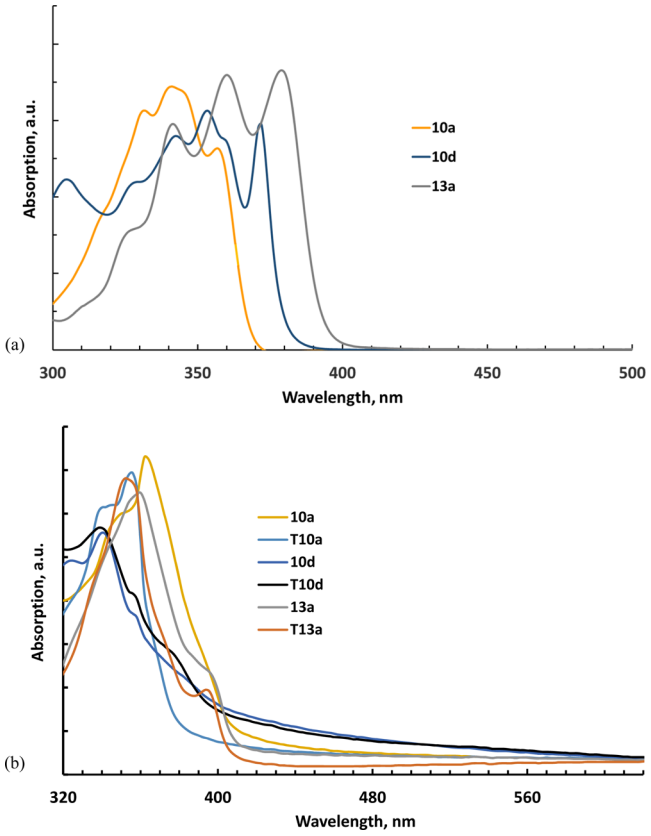

Figure 3. Absorption spectra of (a) diluted solutions of N,S,Se-heteroacenes and (b) solid layers of N,S,Se-heteroacenes and their N,S-counterparts.

with the correlation established for molecular glasses: the lower molecule dipole moment, the lower amplitude of the disorder, and hence, the larger charge carrier mobility of the film.[33] For each couple of selenated and sulfurated molecules, electron density distribution on HOMO levels are similar (for more details, see Table S1) and the somewhat difference in hole mobility is within the experimental error.

The difference between selenated molecules **10d** and **13a** and the sulfurated ones **T-10d** and **T-13a** can also be attributed to π-conjugation, as revealed by the UV spectra in Figures 3 and S28–S29, showing that the spectra of selenated molecules are red-shifted.

One may conclude that the larger the planar area of the studied molecules is, the better the intermolecular $\pi-\pi$ stacking interactions are, and as a consequence, better is the intermolecular electron transfer. Nevertheless, the apparently low mobilities measured using the technique of CELIV can be attributed to the disorder in the polycrystalline thin films under study.[34] The CELIV mobility of the staple-compound spiro-MeOTAD, which is well known as a hole transport layer (HTL), measured under similar conditions was 8.5×10^{-7} $cm^{-2}{\cdot}V^{-1}{\cdot}s^{-1}$,[35] whereas that measured under the ambient condition was 7.2×10^{-4} $cm^{-2}{\cdot}V^{-1}{\cdot}s^{-1}$[36] (for comparison, the mobility obtained from space charge-limited current measurements in diodes was found to be equal to 4×10^{-5}[37] and 1.6×10^{-4} $cm^{-2}{\cdot}V^{-1}{\cdot}s^{-1}$[38]). This makes the reported compounds realistic candidates for HTL in solid-state perovskite based devices as the HOMO-level positions of the heteroacenes match well to the valence band of methylammonium lead iodide ($MAPbI_3$), for instance. Moreover, the lowest unoccupied molecular orbital (LUMO) of each compound is higher than the edge of the conduction band which ranged within −3.7 and −4.0 eV for $MAPbI_3$ and its analogues. Thus, the studied compounds possess the electron blocking capability, another critical parameter of HTL.

CONCLUSIONS

In summary, we presented an effective synthetic approach toward two classes of N,S,Se-heteroacenes with the combination of pyrrole, thiophene, and selenophene rings in their fused scaffolds, namely, BSTI and BSTTI derivatives. Indeed, construction of these fused molecules was readily performed from ethyl 3-bromobenzo[*b*]selenophene-2-carboxylate, available BS-cored material, via the sequence of transition-metal-free reactions, including the Fiesselmann thiophene and Fischer indole synthesis. Semiconductor properties of some herein-obtained BSTI and BSTTI derivatives as well as their analogues, bearing benzo[*b*]thiophene instead of benzo[*b*]-selenophene in the structure, were studied by preparing thin solid films and measuring the charge carrier mobility. CELIV hole mobility of the order of 10^{-5} $cm^2{\cdot}V^{-1}{\cdot}s^{-1}$ estimated for electric field of 10^4 $V{\cdot}cm^{-1}$ makes them potential materials for use as a hole-transporting layer in organic optoelectronic devices. Because their HOMO energy levels match well to the valence band of methylammonium lead iodide and similar perovskites, one may conclude that the studied heteroacenes can be used as HTL in perovskite-based solar cells, photodiodes, and LEDs.

EXPERIMENTAL SECTION

Analytical studies were carried out using the equipment of the Center for Joint Use "Spectroscopy and Analysis of Organic Compounds" at the Postovsky Institute of Organic Synthesis of the Russian Academy of Sciences (Ural Division). Melting points were determined on combined heating stages and are uncorrected. Elemental analysis was carried on an automated

Table 1. Characteristics of Thin Solid Films of N,S,Se-Heteroacenes and Their N,S-Counterparts[a]

compound	λ_{max}, nm	E_g^{opt}, eV	HOMO/LUMO energy level, eV (±1%)	dipole moment, D	hole mobility, $\times 10^{-5}$ $cm^2{\cdot}V^{-1}{\cdot}s^{-1}$ (CI[b] 95%)
10a	362	3.00	−5.52/−2.52	1.73	1.6 ± 0.5
T-10a	356	3.24	−5.60/−2.36	1.60	1.8 ± 0.5
10d	340	2.83	−5.25/−2.42	1.55	3.9 ± 1.2
T-10d	338	3.00	−5.23/−2.23	1.42	3.3 ± 1.0
13a	360; 396	3.01	−5.20/−2.19	2.16	2.4 ± 0.7
T-13a	352; 394	3.04	−5.26/−2.22	2.31	2.0 ± 0.6

[a]Absorption maximum λ_{max} and optical band gap E_g^{opt} are from spectra in Figures 3 and S27–S29. HOMO level is obtained from CV data (Figure S30). LUMO level is calculated from the HOMO using E_g^{opt}. Molecule dipole moment is from DFT calculations (Table S1). Hole mobility corresponds to that at an electric field of ca. 1×10^4 V cm^{-1}. [b]Confidence interval calculated from 10 replicates.

https://dx.doi.org/10.1021/acsomega.0c00383
ACS Omega 2020, 5, 9377−9383

CHN analyzer. Mass spectrometry was performed using a high-resolution Q-TOF LC−MS/MS spectrometer. NMR measurements were performed on NMR spectrometers at 400 and 500 MHz for ^{1}H, 126 MHz for ^{13}C and 471 MHz for ^{19}F spectra in DMSO-d_6 or $CDCl_3$, with tetramethylsilane as an internal standard for ^{1}H, ^{13}C spectra and perfluorobenzene for ^{19}F ones. The^{13}C NMR spectra of some BSTTI (**13b−d**) could not be determined because of poor solubility of these compounds in a majority of deuterated solvents. Unless otherwise stated, all reagents were purchased from commercial sources and used without further purification.

General Procedure for Cyclic Voltammetry. In thin layers of the N,S,Se-heteroacenes, HOMO energy levels were determined by cyclic voltammetry (CV). The CV experiment was carried out at the scan rate of 20 mV/s in a three-electrode three-compartment electrochemical cell in the glove box with a dry argon atmosphere. Platinum sheets served as the working and counter electrodes. A 20 nm solid layer of an examined material was preliminarily deposited onto the working electrode by thermal evaporation of the compound under 10^{-6} mbar vacuum at the rate of 1 Å/s. A 0.2 M solution of tetrabutylammonium hexafluorophosphate (NBu_4PF_6) in acetonitrile (HPLC-grade) was used as an electrolyte. An Ag wire immersed into the electrolyte solution with the addition of 0.1 M $AgNO_3$ was used as a pseudo reference electrode (Ag/Ag^+). It was calibrated against ferrocene/ferricenium couple (0.039 V vs Ag/Ag^+), and its potential was recalculated to the energy scale using 4.988 eV value for Fc/Fc^+ in acetonitrile reported in the literature.[39] Thus, the energy level of Ag/Ag^+ (E_{Ag/Ag^+}) in this case is 5.027 eV. Taking into account the accuracy of the CV experiment (±0.02 V), this value should be rounded to 5.03 eV. For all the substances, we failed to determine the LUMO level because of the rather wide optical band gap that ranged around 2.4−2.6 eV. Therefore, taking into account the determined electrochemical response of the HOMO, the response of the LUMO should lie in the range of potentials near −2.4 V, which is close to the cathodic limit of the electrochemical stability window of acetonitrile.

Charge Carrier Mobility Measurements. In thin solid layers, the charge carrier mobility was measured using the technique of charge extraction by linearly increasing voltage (CELIV).[40] Metal-insulator-semiconductor (MIS) diode structures, similar to those described earlier,[41,42] were prepared. Onto the ITO (indium-tin oxides) electrode of the ITO/glass substrate, a SiO_2 insulator layer of 70 nm in thickness was deposited by conventional magnetron sputtering. Then, a 100 nm layer of the studied N,S,Se-heteroacenes and a 80 nm layer of Au electrode were deposited successively by thermal evaporation of the material under 10^{-6} mbar vacuum at the rate of 1 Å/s. The CELIV setup included a digital USB-oscilloscope (DL-Analog Discovery, Digilent Co.), which played roles of the master pulse generator and transient current pulse monitor. *RC* constants were at least a factor of 20 smaller than the time scales of interest. Small charge extraction regime was used, that is, no injection (offset) voltage was applied in the experiments. The SiO_2 layer blocked injection of charge carries from the ITO electrode.

For all the studied devices, the displacement current $j(0)$ was observed to exceed the maximum drift current Δj, that is, $\Delta j \ll j(0)$, as seen in a typical transient curve presented in Figure 4. Therefore, the charge carrier mobility μ was estimated in accordance with eq 1[40]

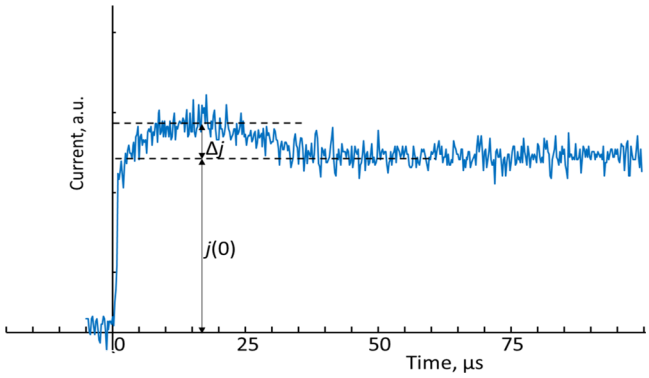

Figure 4. Charge carrier mobility measurements using the CELIV method. Transient current of holes in an ITO/SiO_2/10d/Au structure at $A = 5.6 \times 10^3$ V/s, $t_{max} = 16.7$ μs.

$$\mu = \frac{2d^2}{3At_{max}^2} \quad (1)$$

where d is the film thickness equal to 100 nm, A is the applied voltage ramp in the range 4/10 kV/s, and t_{max} is the time corresponding to the maximum of the current $j(t_{max}) = \Delta j + j(0)$. The mobility data range was 95% confidence interval calculated from 10 replicates for each sample.

Computational Methods. The computations of frontier molecular orbitals, the HOMO and LUMO energy levels, and the dipole moment values were based on restricted density functional theory (DFT).[43−46] Computing was carried out in the Orca 4.0.1 software package using the DFT B3LYP, 6-311G* method.[47]

■ ASSOCIATED CONTENT

Supporting Information

The Supporting Information is available free of charge at https://pubs.acs.org/doi/10.1021/acsomega.0c00383.

Copies of ^{1}H, ^{19}F, and ^{13}C NMR spectra of all new compounds (PDF)

■ AUTHOR INFORMATION

Corresponding Authors

Roman A. Irgashev − *I. A. Postovsky Institute of Organic Synthesis, Ural Division, Russian Academy of Sciences, Ekaterinburg 620990, Russia; Ural Federal University Named after the First President of Russia B.N. Yeltsin, Ekaterinburg 620002, Russia;* orcid.org/0000-0002-8428-1748; Email: irgashev@ios.uran.ru

Alexey R. Tameev − *I. A. Postovsky Institute of Organic Synthesis, Ural Division and A. N. Frumkin Institute of Physical Chemistry and Electrochemistry, Russian Academy of Sciences, Ekaterinburg 620990, Russia;* orcid.org/0000-0001-8865-3361; Email: tameev@elchem.ac.ru

Authors

Nadezhda S. Demina − *I. A. Postovsky Institute of Organic Synthesis, Ural Division, Russian Academy of Sciences, Ekaterinburg 620990, Russia; Ural Federal University Named after the First President of Russia B.N. Yeltsin, Ekaterinburg 620002, Russia;* orcid.org/0000-0002-5475-134X

Nikolay A. Rasputin − *I. A. Postovsky Institute of Organic Synthesis, Ural Division, Russian Academy of Sciences, Ekaterinburg 620990, Russia; Ural Federal University Named*

https://dx.doi.org/10.1021/acsomega.0c00383
ACS Omega 2020, 5, 9377−9383

after the First President of Russia B.N. Yeltsin, Ekaterinburg 620002, Russia; orcid.org/0000-0002-4610-3617

Natalia V. Nekrasova − *A. N. Frumkin Institute of Physical Chemistry and Electrochemistry, Russian Academy of Sciences, Moscow 119071, Russia*

Gennady L. Rusinov − *I. A. Postovsky Institute of Organic Synthesis, Ural Division, Russian Academy of Sciences, Ekaterinburg 620990, Russia; Ural Federal University Named after the First President of Russia B.N. Yeltsin, Ekaterinburg 620002, Russia*

Jean-Michel Nunzi − *Department of Physics, Engineering Physics and Astronomy, Department of Chemistry, Queens University, Kingston, Ontario K7L-3N6, Canada;* orcid.org/0000-0001-5490-4273

Valery N. Charushin − *I. A. Postovsky Institute of Organic Synthesis, Ural Division, Russian Academy of Sciences, Ekaterinburg 620990, Russia; Ural Federal University Named after the First President of Russia B.N. Yeltsin, Ekaterinburg 620002, Russia*

Complete contact information is available at: https://pubs.acs.org/10.1021/acsomega.0c00383

Notes

The authors declare no competing financial interest.

■ ACKNOWLEDGMENTS

The research (synthesis of new heteroacenes and investigation of their semiconductor properties) was financially supported by the Russian Science Foundation (project no. 18-13-00409). N.S.D. and N.A.R. would like to acknowledge the financial support for the analytical studies of synthesized compounds from the Ministry of Education and Science of the Russian Federation within the framework of the State Assignment for Research (project no. AAAA-A19-119012490006-1). The authors are grateful to Grigory A. Kim for carrying out the DFT calculations which were performed using ⟨⟨Uran⟩⟩ supercomputer of the Institute of Mathematic and Mechanics of the Ural Branch of the Russian Academy of Sciences. The XRD measurements were performed using the equipment of CKP FMI IPCE RAS.

■ REFERENCES

(1) Zhu, M.; Yang, C. Blue Fluorescent Emitters: Design Tactics and Applications in Organic Light-Emitting Diodes. *Chem. Soc. Rev.* **2013**, *42*, 4963−4976.

(2) Bhatnagar, P. K. Organic Light-Emitting Diodes—A Review. In *Nanomaterials and Their Applications*; Khan, Z. H., Ed.; Springer: Singapore, 2018; pp 261−287.

(3) Tao, Y.; Yang, C.; Qin, J. Organic Host Materials for Phosphorescent Organic Light-Emitting Diodes. *Chem. Soc. Rev.* **2011**, *40*, 2943−2970.

(4) Zhang, W.; Yu, G. Organic Semiconductors for Field-Effect Transistors. In *Organic Optoelectronic Materials*; Li, Y., Ed.; Springer: Cham, 2015; pp 51−164.

(5) Wang, C.; Dong, H.; Hu, W.; Liu, Y.; Zhu, D. Semiconducting π-Conjugated Systems in Field-Effect Transistors: A Material Odyssey of Organic Electronics. *Chem. Rev.* **2012**, *112*, 2208−2267.

(6) Tong, S.; Sun, J.; Yang, J. Printed Thin-Film Transistors: Research from China. *ACS Appl. Mater. Interfaces* **2018**, *10*, 25902−25924.

(7) Tress, W. Organic Solar Cells. In *Organic Solar Cells*; Tress, W., Ed.; Springer: Cham, 2014; pp 67−214.

(8) Zhang, G.; Zhao, J.; Chow, P. C. Y.; Jiang, K.; Zhang, J.; Zhu, Z.; Zhang, J.; Huang, F.; Yan, H. Nonfullerene Acceptor Molecules for Bulk Heterojunction Organic Solar Cells. *Chem. Rev.* **2018**, *118*, 3447−3507.

(9) Kirchartz, T.; Kaienburg, P.; Baran, D. Figures of Merit Guiding Research on Organic Solar Cells. *J. Phys. Chem. C* **2018**, *122*, 5829−5843.

(10) Liu, Y.; He, K.; Chen, G.; Leow, W. R.; Chen, X. Nature-Inspired Structural Materials for Flexible Electronic Devices. *Chemical Reviews*; American Chemical Society October, 2017; pp 12893−12941.

(11) Tan, Y. J.; Wu, J.; Li, H.; Tee, B. C. K. Self-Healing Electronic Materials for a Smart and Sustainable Future. *ACS Appl. Mater. Interfaces* **2018**, *10*, 15331−15345.

(12) Cai, S.; Han, Z.; Wang, F.; Zheng, K.; Cao, Y.; Ma, Y.; Feng, X. Review on Flexible Photonics/Electronics Integrated Devices and Fabrication Strategy. *Sci. China Inf. Sci.* **2018**, *61*, 060410.

(13) Mu, W.; Sun, S.; Zhang, J.; Jiao, M.; Wang, W.; Liu, Y.; Sun, X.; Jiang, L.; Chen, B.; Qi, T. Advantage of Arch-Shaped Structure on Transistor Performances over Linear-Shaped Structure in Dibenzothienopyrrole Semiconductors. *Org. Electron.* **2018**, *61*, 78−86.

(14) Zhou, F.; Liu, S.; Santarsiero, B. D.; Wink, D. J.; Boudinet, D.; Facchetti, A.; Driver, T. Synthesis and Properties of New N-Heteroheptacenes for Solution-Based Organic Field Effect Transistors. *Chem.—Eur. J.* **2017**, *23*, 12542−12549.

(15) Zhang, X.-H.; Cui, Y.; Katoh, R.; Koumura, N.; Hara, K. Organic Dyes Containing Thieno[3,2-b]Indole Donor for Efficient Dye-Sensitized Solar Cells. *J. Phys. Chem. C* **2010**, *114*, 18283−18290.

(16) Irgashev, R. A.; Karmatsky, A. A.; Kozyukhin, S. A.; Ivanov, V. K.; Sadovnikov, A.; Kozik, V. V.; Grinberg, V. A.; Emets, V. V.; Rusinov, G. L.; Charushin, V. N. A Facile and Convenient Synthesis and Photovoltaic Characterization of Novel Thieno[2,3-b]Indole Dyes for Dye-Sensitized Solar Cells. *Synth. Met.* **2015**, *199*, 152−158.

(17) Huang, Z.-S.; Hua, T.; Tian, J.; Wang, L.; Meier, H.; Cao, D. Dithienopyrrolobenzotriazole-Based Organic Dyes with High Molar Extinction Coefficient for Efficient Dye-Sensitized Solar Cells. *Dyes Pigm.* **2016**, *125*, 229−240.

(18) Cheng, H.; Wu, Y.; Su, J.; Wang, Z.; Ghimire, R. P.; Liang, M.; Sun, Z.; Xue, S. Organic Dyes Containing Indolodithienopyrrole Unit for Dye-Sensitized Solar Cells. *Dyes Pigm.* **2018**, *149*, 16−24.

(19) Jeong, I.; Chae, S.; Yi, A.; Kim, J.; Chun, H. H.; Cho, J. H.; Kim, H. J.; Suh, H. Syntheses and Photovoltaic Properties of 6-(2-Thienyl)-4H-Thieno[3,2-b]Indole Based Conjugated Polymers Containing Fluorinated Benzothiadiazole. *Polymer* **2017**, *109*, 115−125.

(20) Yamamoto, T.; Takimiya, K. Facile Synthesis of Highly π-Extended Heteroarenes, Dinaphtho[2,3-b:2′,3′-f]Chalcogenopheno[3,2-b]Chalcogenophenes, and Their Application to Field-Effect Transistors. *J. Am. Chem. Soc.* **2007**, *129*, 2224−2225.

(21) Kong, H.; Jung, Y. K.; Cho, N. S.; Kang, I.-N.; Park, J.-H.; Cho, S.; Shim, H.-K. New Semiconducting Polymers Containing 3,6-Dimethyl(Thieno[3,2- b]Thiophene or Selenopheno[3,2- b]-Selenophene) for Organic Thin-Film Transistors. *Chem. Mater.* **2009**, *21*, 2650−2660.

(22) Izawa, T.; Miyazaki, E.; Takimiya, K. Solution-Processible Organic Semiconductors Based on Selenophene-Containing Heteroarenes, 2,7-Dialkyl[1]Benzoselenopheno[3,2- b][1]-Benzoselenophenes (C_n BSBSs): Syntheses, Properties, Molecular Arrangements, and Field-Effect. *Chem. Mater.* **2009**, *21*, 903−912.

(23) Hollinger, J.; Gao, D.; Seferos, D. S. Selenophene Electronics. *Isr. J. Chem.* **2014**, *54*, 440−453.

(24) Arsenyan, P.; Petrenko, A.; Leitonas, K.; Volyniuk, D.; Simokaitiene, J.; Klinavičius, T.; Skuodis, E.; Lee, J.-H.; Gražulevičius, J. V. Synthesis and Performance in OLEDs of Selenium-Containing Phosphorescent Emitters with Red Emission Color Deeper Than the Corresponding NTSC Standard. *Inorg. Chem.* **2019**, *58*, 10174−10183.

(25) Ghosh, S.; Bedi, A.; Zade, S. S. Thienopyrrole and Selenophenopyrrole Donor Fused with Benzotriazole Acceptor: Microwave Assisted Synthesis and Electrochemical Polymerization. *RSC Adv.* **2015**, *5*, 5312−5320.

(26) Ghosh, S.; Das, S.; Kumar, N. R.; Agrawal, A. R.; Zade, S. S. Effect of Heteroatom (S/Se) Juggling in Donor−Acceptor−Donor (D−A−D) Fused Systems: Synthesis and Electrochemical Polymerization. *New J. Chem.* **2017**, *41*, 11568−11575.
(27) Mishra, S. P.; Javier, A. E.; Zhang, R.; Liu, J.; Belot, J. A.; Osaka, I.; McCullough, R. D. Mixed Selenium-Sulfur Fused Ring Systems as Building Blocks for Novel Polymers Used in Field Effect Transistors. *J. Mater. Chem.* **2011**, *21*, 1551−1561.
(28) Mori, T.; Nishimura, T.; Yamamoto, T.; Doi, I.; Miyazaki, E.; Osaka, I.; Takimiya, K. Consecutive Thiophene-Annulation Approach to π-Extended Thienoacene-Based Organic Semiconductors with [1]Benzothieno[3,2- b][1]Benzothiophene (BTBT) Substructure. *J. Am. Chem. Soc.* **2013**, *135*, 13900−13913.
(29) Irgashev, R. A.; Karmatsky, A. A.; Rusinov, G. L.; Charushin, V. N. Construction of Heteroacenes with Fused Thiophene and Pyrrole Rings via the Fischer Indolization Reaction. *Org. Lett.* **2016**, *18*, 804−807.
(30) Irgashev, R. A.; Steparuk, A. S.; Rusinov, G. L. A New Convenient Synthetic Route towards 2-(Hetero)Aryl-Substituted Thieno[3,2- b]Indoles Using Fischer Indolization. *Org. Biomol. Chem.* **2018**, *16*, 4821−4832.
(31) Paegle, E.; Belyakov, S.; Arsenyan, P. An Approach to the Selenobromination of Aryl(Thienyl)Alkynes: Access to 3-Bromobenzo[b]Selenophenes and Selenophenothiophenes. *Eur. J. Org. Chem.* **2014**, 3831−3840.
(32) Paegle, E.; Belyakov, S.; Petrova, M.; Liepinsh, E.; Arsenyan, P. Cyclization of Diaryl(Hetaryl)Alkynes under Selenobromination Conditions: Regioselectivity and Mechanistic Studies. *Eur. J. Org. Chem.* **2015**, 4389−4399.
(33) Novikov, S. V.; Dunlap, D. H.; Kenkre, V. M. Charge-Carrier Transport in Disordered Organic Materials: Dipoles, Quadrupoles, Traps, and All That. *Proc. SPIE-Int. Soc. Opt. Eng.* **1998**, *3471*, 181−191.
(34) Nikitenko, V. R.; Amrakulov, M. M.; Khan, M. D. Theory of the Anomalous Diffusion of Carriers in Disordered Organic Materials under Conditions of the CELIV Experiment. *Semiconductors* **2016**, *50*, 435−439.
(35) Aukštuolis, A.; Girtan, M.; Mousdis, G. A.; Mallet, R.; Socol, M.; Rasheed, M.; Stanculescu, A. Measurement of Charge Carrier Mobility in Perovskite Nanowire Films by Photo-Celiv Method. *Proc. Rom. Acad. Math. Phys. Tech. Sci. Inf. Sci.* **2017**, *18*, 34−41.
(36) Liu, Y.; Zhang, H.; Zhang, Y.; Xu, B.; Liu, L.; Chen, G.; Im, C.; Tian, W. Influence of Hole Transport Layers on Internal Absorption, Charge Recombination and Collection in HC(NH2)2PbI3 Perovskite Solar Cells. *J. Mater. Chem. A* **2018**, *6*, 7922−7932.
(37) Leijtens, T.; Ding, I.-K.; Giovenzana, T.; Bloking, J. T.; McGehee, M. D.; Sellinger, A. Hole Transport Materials with Low Glass Transition Temperatures and High Solubility for Application in Solid-State Dye-Sensitized Solar Cells. *ACS Nano* **2012**, *6*, 1455−1462.
(38) Snaith, H. J.; Grätzel, M. Enhanced Charge Mobility in a Molecular Hole Transporter via Addition of Redox Inactive Ionic Dopant: Implication to Dye-Sensitized Solar Cells. *Appl. Phys. Lett.* **2006**, *89*, 262114.
(39) Namazian, M.; Lin, C. Y.; Coote, M. L. Benchmark Calculations of Absolute Reduction Potential of Ferricinium/Ferrocene Couple in Nonaqueous Solutions. *J. Chem. Theory Comput.* **2010**, *6*, 2721−2725.
(40) Mozer, A. J.; Sariciftci, N. S.; Pivrikas, A.; Österbacka, R.; Juška, G.; Brassat, L.; Bässler, H. Charge Carrier Mobility in Regioregular Poly(3-Hexylthiophene) Probed by Transient Conductivity Techniques: A Comparative Study. *Phys. Rev. B: Condens. Matter Mater. Phys* **2005**, *71*, 035214.
(41) Malov, V. V.; Ghosh, T.; Nair, V. C.; Maslov, M. M.; Katin, K. P.; Unni, K. N. N.; Tameev, A. R. Hole Mobility in Thieno[3,2-b]Thiophene Oligomers. *Mendeleev Commun.* **2019**, *29*, 218−219.
(42) Irgashev, R. A.; Kazin, N. A.; Makarova, N. I.; Dorogan, I. V.; Malov, V. V.; Tameev, A. R.; Rusinov, G. L.; Metelitsa, A. V.; Minkin, V. I.; Charushin, V. N. Synthesis and Properties of New π-Conjugated Imidazole/Carbazole Structures. *Dyes Pigm.* **2017**, *141*, 512−520.
(43) Krishnan, R.; Binkley, J. S.; Seeger, R.; Pople, J. A. Self-Consistent Molecular Orbital Methods. XX. A Basis Set for Correlated Wave Functions. *J. Chem. Phys.* **1980**, *72*, 650−654.
(44) McLean, A. D.; Chandler, G. S. Contracted Gaussian Basis Sets for Molecular Calculations. I. Second Row Atoms, Z=11-18. *J. Chem. Phys.* **1980**, *72*, 5639−5648.
(45) Clark, T.; Chandrasekhar, J.; Spitznagel, G. n. W.; Schleyer, P. V. R. Efficient Diffuse Function-augmented Basis Sets for Anion Calculations. III. The 3-21+G Basis Set for First-row Elements, Li−F. *J. Comput. Chem.* **1983**, *4*, 294−301.
(46) Frisch, M. J.; Pople, J. A.; Binkley, J. S. Self-Consistent Molecular Orbital Methods 25. Supplementary Functions for Gaussian Basis Sets. *J. Chem. Phys.* **1984**, *80*, 3265−3269.
(47) Neese, F. The ORCA Program System. *Wiley Interdiscip. Rev.: Comput. Mol. Sci.* **2012**, *2*, 73−78.

https://dx.doi.org/10.1021/acsomega.0c00383
ACS Omega 2020, 5, 9377−9383